IJE TRANSACTIONS B: Applications Vol. 35, No. 05, (May 2022) 954-966

International Journal of Engineering

Journal Homepage: www.ije.ir

Use of Random Vortex Method in Simulating Non-Newtonian Fluid Flow in a T-junction for Various Reynolds Numbers and Power-law Indexes

Y. Noori[a], A. R. Teymourtash*[a], B. Zafarmand[b]

[a] *Department of Mechanical Engineering, Faculty of Engineering, Ferdowsi University of Mashhad, Mashhad, Iran*

[b] *Department of Mechanical Engineering and Power Plant, Khorasan Water and Power Industry Higher Educational and Research Complex, Mashhad, Iran*

PAPER INFO

Paper history:
Received 08 January 2022
Received in revised form 09 February 2022
Accepted 09 February 2022

Keywords:
Random Vortex Method
Non-Newtonian
power-law Fluid
T-junction
Navier-Stokes Equations
Schwarz-christoffel Conformal Mapping

ABSTRACT

Past studies show that until now the Random Vortex Method (RVM) has only been used to solve the flow of Newtonian fluids. In this paper, by presenting a new approach, the RVM is developed for the first time with the aim of simulating the flow of non-Newtonian fluids. For this purpose, a numerical simulation of two-dimensional flow of non-Newtonian power-law fluid in a T-junction is presented. The simulation is conducted for *Re = 50-200* at the inlet of the channel and different power-law indexes (*n = 0.2-1.4*). The RVM solves the Navier–Stokes equations as a function of time and determines the velocity at any point of the channel directly and without determining a mesh on the geometry. Potential velocity, an initial condition for the flow analysis by the RVM, is obtained using the Schwarz–Christoffel conformal mapping. The effect of two parameters of power-law index and Reynolds number on the recirculation zone has been investigated. Acceptable agreement among the results of the present study and the existing numerical and experimental results shows the capability of the proposed method, according to which the RVM can be considered a powerful promising method in simulating the non-Newtonian fluids in laminar and turbulent flow regimes.

***doi**: 10.5829/ije.2022.35.05b.11*

NOMENCLATURE

U	inlet velocity of the channel (m/s)	b	heterogeneous source term in the vorticity equation
H	inlet height of the channel (m)	$Gr(x,t)$	Green function
n	power-Law index	Δt	time step (s)
m	power-Law consistency index	Re	Reynolds number at the inlet section of the channel
Q_1	inlet flow rate of the channel (m^3/s)	Re_r	local Reynolds number
Q_2	outlet flow rate from the longitudinal branch (m^3/s)	u_x	velocity profile in x direction (m/s)
Q_3	outlet flow rate from the lateral branch (m^3/s)	u_{ave}	average velocity (m/s)
z	complex number on z-plane	L_r	recirculation length (m)
t	complex number on t-plane	**Greek Symbols**	
$\bar{t}$	conjugate of t	∇	Del operator
dt/dz	Schwarz-Christoffel transfer function	μ	dynamic viscosity (pa.s)
N	total number of vortexes	ω^*	dimensionless vorticity in normal direction to the x-y plane
$F(t_j)$	Schwarz-Christoffel transfer function	ρ	fluid density (kg/m^3)
$\overline{W}(z_j)$	induced velocity equation on the vortex j	σ	standard deviation of Gaussian distribution
t^*	dimensionless time	$\dot{\gamma}$	shear rate (s^{-1})
V^*	dimensionless velocity vector	$\dot{\gamma}^*$	dimensionless shear rate
x^*	x-dimensionless coordinates	μ_a	apparent viscosity (pa.s)
y^*	y-dimensionless coordinates	ω	vorticity in normal direction to the x-y plane (s^{-1})
u^*	dimensionless velocity in x direction	**Superscript**	
v^*	dimensionless velocity in y direction	*	dimensional variable

*Corresponding Author Institutional Email: *teymourtash@um.ac.ir* (A. R. Teymourtash)

Please cite this article as: Y. Noori, A. R. Teymourtash, B. Zafarmand, Use of Random Vortex Method in Simulating Non-Newtonian Fluid Flow in a T-junction for Various Reynolds Numbers and Power-law Indexes, ***International Journal of Engineering, Transactions B: Applications***, Vol. 35, No. 05, (2022) 954-966

1. INTRODUCTION

One of the most promising and accurate methods for studying the viscous flow in the laminar and turbulent regimes, is the Random Vortex Method (RVM). So far, all studies performed with this method are limited to Newtonian fluids. However, the behavior of most real fluids used in the food, petroleum and petrochemical industries, such as solutions and molten polymers, industrial oils, as well as materials that have viscous and elastic properties (viscoelastic) is considered non-Newtonian, and because of its wide application in industry, it is a topic that is always discussed and various methods are used to study and simulate such process.

Numerous methods for studying and modeling non-Newtonian fluid flow have been discovered and identified. Each has proven its strengths and weaknesses through repeated research. But, what is certain is that the discovery and appearance of an accurate method to simulate fluid flow has always been of interest. For this reason, this paper develops the RVM in order to simulate the flow of non-Newtonian fluids by introducing a new approach for the first time. For this purpose, the non-Newtonian power-law fluid in a T-junction is simulated using RVM.

The T-junctions are often used as phase separators for raw materials (liquid-gas) in industrial applications such as refrigeration system, advanced thermodynamic cycle, nuclear reactors, petroleum exploitation pipelines and so on [1]. More applications of T-junction have been mentioned in the research of Yang et al. [1]. The junctions (T or Y) are commonly located in such a way that the inlet two-phase flow to the branch is unequal separated between the side and main branches, and puts the gas-rich flow in the side branch and the liquid-rich flow in the main branch.

In the RVM, a limited number of vortexes are generated and are followed in the form of a numerical algorithm using the Lagrangian perspective. To solve the unsteady flow, each time step is divided into two half steps. In the first half step, the effects of the viscosity are neglected and this time step is passed by the convection mechanism. In the second half step, the viscosity effects are influenced by the random movement of the vortex bubbles generated by the diffusion mechanism.

RVM is employed to solve the two-dimensional equations of motion and the time function of incompressible fluids in laminar and turbulent flows. The method is based on solving the time-dependent vorticity equation, which is obtained from the effect of the Curl operator on the Navier-Stokes equations and its integration with the continuity equation.

The condition of no-slip on the wall at any point in time is the boundary condition for solving the fluid flow equations. In the RVM, to reduce the wall velocity tangential component to zero, a number of definite constant rotational vortexes are produced and their movements are generated due to both mechanisms of convection, diffusion and Lagrangian perspective accordingly. The motion of each vortex stems from the potential velocity of the fluid in addition to the total instantaneous velocities induced by the other vortexes and their images at the center of the intended vortex. Similarly, the instantaneous velocity at any point in the field is obtained using the instantaneous velocities induced by the vortexes, their images, and the velocity of the potential velocity passing through that point.

The RVM was first introduced by Alexandre Chorin who proposed a model for turbulent flow around a cylinder in 1973 [2]. He modified this method in 1978 to import the boundary conditions to the calculations for the boundary layer analysis, and named it the Random Vortex Method [3]. Thereafter, RVM became known as a numerical method for solving the flow field.

Gagnon and Giovannini [4] were other people who did their research using the RVM. In this study numerical simulation and physical analysis of high Reynolds number recirculating flows behind sudden expansions have been investigated.

Many researchers have recently done their investigation using RVM, some of which are mentioned here. Noori and Zafarmand [5] simulated the laminar and turbulent flow inside some divergent channels and investigated the effects of the divergence angle and Reynolds number on the reverse flow inside the channel using RVM. In this study, the flow inside divergent channels with different angles and Reynolds numbers was investigated; while, instantaneous and average velocities being calculated. A demonstration of the production of vortexes and their distribution was presented. The movement of the produced vortexes instantly and at different times was well depicted. In addition to the above results in this study, the effect of divergence angle and Reynolds number on flow separation within divergent channels was investigated and the results are presented in a useful graph.

Zafarmand et al. [6] studied the turbulent flow in a channel using the vortex blob method. They obtained and discussed the physical concepts of turbulence and entropy generation. At first, time-averaged velocities and then their fluctuations were calculated. It was observed that turbulence structures occupy different positions and move with convection velocity. To verify the second law of thermodynamics, averaged vorticity and its fluctuations as well as averaged entropy and its fluctuations were calculated. In this research, for the first time, the turbulence structures were visualized and presented by employing the vector of velocity fluctuations, vorticity and entropy generation fluctuations.

Zafarmand and Ghadirzad [7] studied high Reynolds viscous flow simulation past a cylinder as well as an elliptical airfoil by random vortex blob. In both cases, the obtained mean time velocities were compared with available numerical and experimental results. Having known the velocity field, by employing momentum balance, the drag and lift coefficients caused by flow past the elliptical airfoil with different diameter ratios were calculated.

Tadayoni-Navaei and Zafarmand [8] used the RVM for geometries with the unsolvable Schwarz-Christoffel formula. In this paper, the Schwarz-Christoffel mapping function for a square cavity is numerically obtained. Then, the instantaneous and the average velocity fields were calculated inside the cavity using the RVM. The advantage of this modeling is that for calculation of velocity at any point of the geometry. There is no need to use meshing in the entire flow field and the velocity in a special point can be obtained directly; also, no need to the other points.

Jin et al. [9] suggested a circle theorem technique to handle 2-D flows around arbitrary cylinders in discrete vortex method. In this work, a novel boundary method is proposed based on the circle theorem technique. Under this algorithm, the identical vortices were introduced outside the body to counteract the lost strengths of vortices through the use of the circle theorem and surface curvature. A series of numerical simulations of flow over various cross-sectional bodies at high Reynolds numbers were performed to validate the accuracies in predicting the hydrodynamic loads, including flow past elliptic, foil, square, and triangular cylinders.

Mimeau et al. [10] compared the semi-Lagrangian Vortex Method (VM) and Lattice Boltzmann Method (LBM) for incompressible flows. In this study, a proven version of each method was used and compared on different three dimensional benchmarks in terms of numerical accuracy, convergence, numerical diffusion and dissipation. It was shown that both methods converge to the same solution but in a different way. The VM performs better than the LBM for the lowest resolution whereas LBM appears to be more accurate for the growing resolutions.

Qian and Yao [11] studied the McKean–Vlasov type stochastic differential equations (SDEs) arising from the random vortex method, which arise from the random vortex dynamics and other physics models. By introducing a new approach, they resolved the existence and uniqueness of both the weak and strong solutions for the McKean–Vlasov stochastic differential equations whose coefficients are defined in terms of singular integral kernels such as the Biot–Savart kernel.

Extensive studies have been performed on T-junctions as well as non-Newtonian fluids. Hayes et al. [12] studied the flow specification of a Newtonian fluid in a two-dimensional, planar, right angled Tee branch by solving the Navier-Stokes equations. In this work the effects of the branch length and the grid size on the interior flow field were examined to assess the accuracy of the solutions. They concluded that the length of the side branch has very little influence on the interior flow field, particularly at higher Reynolds number.

Khandelwal et al. [13] studied the treatment of power-law fluid in a T-channel in the laminar regime. The two-dimensional numerical calculations have been done using Ansys Fluent. In this paper the parameters such as wake length, critical Reynolds number and the variation of viscosity were calculated by using constant density and non-Newtonian power-law viscosity model. The results showed that for a particular power-law index (n), length of recirculation zone increases in the side branch with increasing Re. Also, it increases with decreasing n for the fixed Re. The critical Reynolds number decreases with decreasing n.

Brandi et al. [14] carried out research using the Direct Numerical Simulation (DNS) and Linear Stability Theory (LST) analysis on an Oldroyd-B fluid flowing between two parallel plates. In this paper, the laminar-turbulent transition was studied and the convection of Tollmien–Schlichting waves was investigated for the incompressible, two-dimensional flow between two parallel plates. The viscoelastic fluid adopted was modeled by the Oldroyd-B constitutive equation. DNS and LST were used to verify the stability of the viscoelastic fluid flow to unsteady disturbances.

Zhou et al. [15] examined the dynamics and interfacial evolution for bubble breakup in shear-thinning, non-Newtonian fluids in a microfluidic T-junction. The result showed that the length of the bubble tip is linearly stretched with time, and the elongation rate increases with the concentration of CMC solution. Also, the rheological property of the CMC solution could significantly affect the bubble breakup process in the microfluidic T-junction.

Kwak and Nam [16] presented a simple factor for the vortex formation in power-law fluids flowing inside a channel. Their research explored the feasibility of applying the flow reversal condition on the Couette–Poiseuille (C–P) power-law fluid to predict the vortex generation.

Luo et al. [17] presented the results of mixing the non-Newtonian inelastic fluids in a turbulent patch of T-junction. Results were obtained based on a Direct Numerical Simulation (DNS) of a turbulent flow in a converging T-junction for both Newtonian (water) and non-Newtonian inelastic fluid (dilute Xanthan Gum solution). Based on experimental data, the Bird-Carreau law was used to capture the inelastic shear thinning property of the solution and passive scalar was introduced in the transverse branch to investigate the mixing in such configuration.

Yang et al. [18] carried out an experimental investigation to compare the phase separation performance between the single and double branching T-junctions. The experimental data were compared with the predicted values produced by theoretical models based on water-air mixture, and they found out that there is no suitable model for the refrigerants. It was concluded that the inlet mass flux has little influence on phase separation while the phase separation efficiency drops sharply with the increase of inlet quality.

Rostami and Morini [19] experimentally studied the production of the Newtonian droplets with non-Newtonian and Newtonian bearer flows inside the micro T-junctions. In this paper the generation of Newtonian microdroplets in both Newtonian and non-Newtonian carrier fluids through a commercial micro T-junction under an opposed-flow configuration was analyzed experimentally.

Moghimi et al. [20] examined the effect of non-uniform magnetic field on non-Newtonian fluid separation in a diffuser. The purpose of this study is to investigate the boundary layer separation point in a magnetohydrodynamics diffuser. As an innovation, the Re value on the separation point is determined for the non-Newtonian fluid flow under the influence of the non-uniform magnetic field due to an electrical solenoid, in an empirical case. The impact of the magnetic field intensity on the separation point analyzed from the physical point of view. It was observed the wall shear stress increases by increasing magnetic field intensity that leads to delaying the boundary layer separation.

Maurya et al. [21] examined the combined effects of the power-law rheology and isothermal rotating cylinder on the characteristics of the power-law fluid flow inside the T-junctions. The range of parameters considered in this work is as: Reynolds number, $1 < Re \leq 50$, power-law index, $0.2 \leq n \leq 1$, Prandtl number, $10 \leq Pr \leq 100$ and non-dimensional circumferential velocity of the cylinder, $-5 \leq \alpha \leq 5$. Results suggest that the rotating cylinder can be used as a technique to create and/or reduce the formation of momentum and thermal boundary layers in the flow domain.

Motahar [22] estimated non-Newtonian behavior of nanofluid phase change material containing mesoporous silica particles using a neural network approach. In this paper, the rheological properties of nanofluid phase change material containing mesoporous silica nanoparticles are predicted by the artificial neural networks (ANNs) method based on the experimental database reported in literature. The results showed that the developed ANN has a very low mean squared error for the training and test dataset. Also, the predicted dynamic viscosity and shear stress also have the maximum relative error of 6.26 and 0.418%, respectively.

Vatani and Domiri-Ganji [23] experimentally studied the patterns of the two-phase flow (gas-liquid) inside a rectangular channel with 90° bend. The aim of this study was to analyze the behavior of two-phase flow in an inclined rectangular channel with 90° bend for various vertical lengths. The fluids used in this study were air and water. In this study, the effects of vertical length on flow regimes and pattern transition borders are examined. According to the flow visualization, no vortex was observed in the vertical section. The results showed that the flow regime in the vertical section is churn flow regime. Finally, it can be seen that the flow pattern structures are not greatly affected by changing the vertical length.

In the continuation, this research uses the RVM to simulate the non-Newtonian fluid flow following a new approach for the first time. The target of this research is to develop the RVM in the non-Newtonian fluids simulation. For this purpose, the non-Newtonian power-law fluid in a T-junction is simulated using RVM for *Re=50-200* at the inlet of the channel and different power-law indexes (*n=0.2-1.4*).

2. CONFIGURATION OF THE CASE GEOMETRY AND FINDING THE POTENTIAL VELOCITY

Figure 1 shows a channel with the specifications. The inlet velocity of the channel is *U*, and the inlet height of the channel is *H*. Q_1, Q_2 and Q_3 are the input flow rate, the output flow rate from the longitudinal branch and the output flow rate from the lateral branch, respectively.

Since potential flow analysis for complicated geometries is a very difficult process, the mentioned geometries can be simplified using the conformal mapping. In this approach, a complicated geometry in the z-plane is transformed to a simpler geometry in the t-plane. The Schwartz-Christoffel conformal transfer is used to compute the potential velocity in internal flows. The transformation converts the channel and its inner region, which is located on the z-plane axis, into the upper half of the transfer t-plane axis.

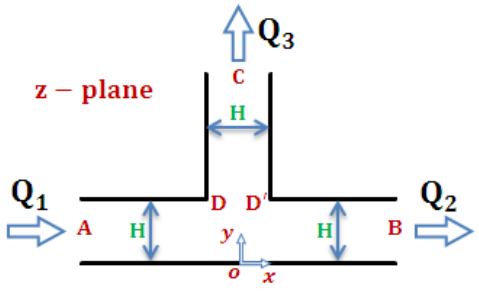

Figure 1. Configuration of channel with a T-junction

The conversion of the channel shown in Figure 1 by the Schwartz-Christofel conformal mapping to its corresponding *t* transfer plane is illustrated in Figure 2.

As mentioned before, to find the potential flow as an initial condition, the Schwartz-Christofel transfer function is used, which is obtained for a T-junction as shown in Equation (1) [25]:

$$\frac{dt}{dz}=\pi\frac{1-t^2}{\sqrt{5-t^2}} \tag{1}$$

According to Figure 2, the input flow to the channel is equivalent to one source and the output flows from the channel are equivalent to two sinks in the complex transfer t-plane.

3-THE GOVERNING EQUATIONS

The governing equation in RVM is the two-dimensional vorticity transport equation where its dimensionless form for the incompressible non-Newtonian fluid flow is derived as follows:

$$\frac{\partial\omega^*}{\partial t^*}+\left(V^*.\nabla\right)\omega^*=\frac{1}{Re}\nabla^2\omega^*+b\left(x,y,t\right) \tag{2}$$

$$\begin{aligned}b=&\frac{\partial\mu}{\partial x^*}\left(\frac{\partial^2 v^*}{\partial x^{*2}}+\frac{\partial^2 v^*}{\partial y^{*2}}\right)-\frac{\partial\mu}{\partial y^*}\left(\frac{\partial^2 u^*}{\partial x^{*2}}+\frac{\partial^2 u^*}{\partial y^{*2}}\right)\\&+\left(\frac{\partial^2\mu}{\partial x^{*2}}-\frac{\partial^2\mu}{\partial y^{*2}}\right)\left(\frac{\partial u^*}{\partial y^*}+\frac{\partial v^*}{\partial x^*}\right)\\&-2\frac{\partial^2\mu}{\partial y^*\partial x^*}\left(\frac{\partial u^*}{\partial x^*}-\frac{\partial v^*}{\partial y^*}\right)+\frac{\partial\mu}{\partial x^*}\frac{\partial\omega^*}{\partial x^*}+\frac{\partial\mu}{\partial y^*}\frac{\partial\omega^*}{\partial y^*}\end{aligned} \tag{3}$$

In the above relations, u^* and v^* are the fluid velocity in x and y directions respectively, μ is the dynamic viscosity and ω^* is the vorticity in normal direction to the x-y plane. b is the heterogeneous term of the source term in the vorticity equation, which becomes to zero ($b=0$) for the Newtonian fluid. Furthermore, Re is the liquid phase Reynolds number at the inlet section of the channel which is derived for the non-Newtonian fluid flow as follows [26]:

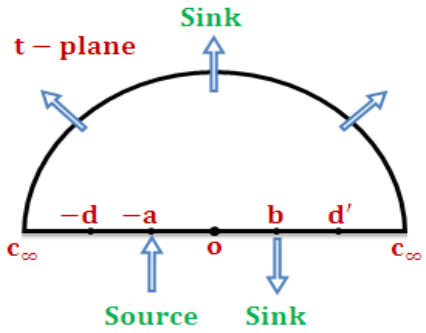

Figure 2. Transmission t-plane for the T-junction

$$Re=\frac{\rho H^{n}U^{2-n}}{m} \tag{4}$$

where ρ is the density of fluid, H is the inlet height of the channel, U is the inlet velocity of the channel, n is the Power-law index and m is the consistency index.

The RVM scheme is based on the vorticity transport equation solution in two steps of convection and diffusion which for non-Newtonian flow, these two steps will be as follows, respectively [4]:

$$\frac{\partial\omega^*}{\partial t^*}+V^*.\nabla\omega^*=0 \tag{5}$$

$$\frac{\partial\omega^*}{\partial t^*}=\frac{1}{Re}\nabla^2\omega^*+b \tag{6}$$

The general solution of the vorticity transport equation is obtained by the summation of the above equations. In the RVM, the no-slip condition or zero relative velocity on the wall at any moment is considered as a boundary condition of the fluid flow equations. In order to zero the sliding velocity on the walls, a number of similar vortexes with the same circulation are generated, and are separated from the wall by the diffusion mechanism and enter the flow field. In the next step, these vortexes continue their motion by both diffusion and convection mechanisms. In addition, to eliminate the normal induced velocity by the vortexes, the vortexes image is used.

To solve the diffusion equation, the Green function is used. According to Andrei Polyanin solution [27], the Green function of Equation (6) is:

$$Gr\left(x,t\right)=\left(\frac{Re}{4\pi t}\right)^{1/2}\exp\left(-\frac{Re}{4t}x^2\right) \tag{7}$$

According to the above relation, the derived Green functions in Newtonian and non-Newtonian fluids are similar. This means that in the non-Newtonian fluid, as in a Newtonian fluid, the diffusion mechanism can be solved using the random perpendicular motion. The motion due to the diffusion of the vortexes is as two perpendicular displacements which are the random variables with Gaussian distribution and a mean value of zero and a standard deviation of $\sigma=\sqrt{\frac{2\Delta t}{\mathrm{Re}}}$ (Δt is the time step).

As a matter of fact, term b has its effects on the standard deviation σ. The effect of adding b to the diffusion equation for a non-Newtonian fluid (despite the same Green functions) could be simulated by an alternative approach. According to this approach, for a non-Newtonian power-law fluid, after calculating the shear rate and apparent viscosity in each time step for any location of the vortex, the local Reynolds and its standard deviation ($\sigma=\sqrt{\frac{2\Delta t}{\mathrm{Re}_r}}$); where Re_r is the local Reynolds in

any point of fluid, are determined for a random motion. In other words, in this approach, it is assumed that for a non-Newtonian fluid in each time step, each point of the fluid that indicates the position of a vortex has different viscosity. To determine the apparent viscosity, after finding the instantaneous velocities of u^* and v^* at any point of the geometry using the RVM, according to power-law model, the shear rate could be computed by the following relations [26]:

$$\dot{\gamma} = \sqrt{2\left(\frac{\partial u}{\partial x}\right)^2 + 2\left(\frac{\partial v}{\partial y}\right)^2 + \left(\frac{\partial u}{\partial y} + \frac{\partial v}{\partial x}\right)^2} = \frac{U}{H}\sqrt{2\left(\frac{\partial u^*}{\partial x^*}\right)^2 + 2\left(\frac{\partial v^*}{\partial y^*}\right)^2 + \left(\frac{\partial u^*}{\partial y^*} + \frac{\partial v^*}{\partial x^*}\right)^2} = \frac{U}{H}\dot{\gamma}^* \tag{8}$$

where $\dot{\gamma}$ is the shear rate. In the power-law model, μ_a is the apparent viscosity which is derived as follows [26]:

$$\mu_a = m\dot{\gamma}^{n-1} = m\left(\frac{U}{H}\dot{\gamma}^*\right)^{n-1} \tag{9}$$

where $\dot{\gamma}^*$ is the dimensionless shear rate, n is the power-law index and m is the consistency index. Now, a relation can be derived between the local Reynolds and the liquid flow Reynolds number at the inlet of the channel as follows:

$$Re_r = \frac{\rho UH}{\mu_a} = \frac{\rho UH}{m\left(\frac{U}{H}\dot{\gamma}^*\right)^{n-1}} = \frac{\rho U^{2-n}H^n}{m}\frac{1}{\dot{\gamma}^{*n-1}} = \frac{Re}{\dot{\gamma}^{*n-1}} \tag{10}$$

In this equation, Re_r is the local Reynolds number and Re is the Reynolds number at the inlet of channel, which in this study is *Re=50-200*. After calculating the fluid shear rate in each time step for each point inside each vortex locations, the local Reynolds and the standard deviation $\sigma = \sqrt{\frac{2\Delta t}{Re_r}}$ for a random motion is determined. In other words, in fluid flow simulation using RVM, the difference between the non-Newtonian and Newtonian fluids is the random motion of the vortexes. In Newtonian fluid, all vortexes in every time step move with the same constant standard deviation. Whereas, for a non-Newtonian fluid, each vortex in each time step performs its random motion with a determined standard deviation and at the same time different.

According to RVM, if N is the total number of vortexes, the induced velocity equation is shown below [5]:

$$\overline{w}\left(z_j\right) = \left[\sum_{\substack{i=1 \\ i\neq j}}^{N} w\left(t_j, t_i\right) - \sum_{i=1}^{N} w\left(t_j, \overline{t}_i\right) + w_p\left(t_j\right)\right] F\left(t_j\right) \tag{11}$$

In this equation, the first term is the set of velocities induced by all vortexes on the vortex j. The second term is the set of velocities induced by the images of all vortexes on the vortex j, and the third term is the velocity of the passing potential at point t_j corresponding to point z_j. Also, t is the complex coordinate in the transfer plane, $\overline{t}$ is the conjugate of t, and $F(t_j)$ is also a Schwarz-Christoffel transfer function.

4. VALIDATION OF RESULTS

To validate the results of this research and indicate the ability of the presented method, first the non-Newtonian flow between two infinite parallel flat plates is solved by RVM and was compared with analytical results. Also, the results of the present study were compared with the results of Hayes et al. [12] and Khandelwal et al. [13].

Consider a unidirectional non-Newtonian flow between two infinite parallel flat plates in the x direction, which located at $y=\pm H/2$. The velocity field u_x, normalized by the mean velocity is given by Rakotomalala et al. [28]:

$$\frac{u_x(y)}{u_{ave}} = \frac{2n+1}{n+1}\left[1 - \left(\frac{2|y|}{H}\right)^{\frac{n+1}{n}}\right] \tag{12}$$

where n represents the Power-law index. The comparison between the analytical solution and the present results for a non-Newtonian flow between two infinite parallel flat plates with different power-law indexes is illustrated in Figure 3. According to this figure, there is a very good conformation between the presented method results and the analytical solution. Figure 4 shows the horizontal velocity profiles between two plates for various power-law indexes resulting from the recent study. For the identical flow rate, when $n>1$ (shear thickening fluid) the profile of velocity becomes sharper. Whereas, when $n<1$ (shear thinning fluid) the profile of velocity changes to plug flow profile.

To validate the present method in solving non-Newtonian flow, the output results have been compared with numerical and experimental results by Hayes et al. [12] and Khandelwal et al. [13]. This comparison is performed for the recirculation length L_r inside the side branch of the T-junction which is studied as the dimensionless ratio of L_r/H (H is the inlet height of the channel) for various power-law indexes ($n=0.2, 0.4, 0.6$ and 1) at different Reynolds numbers. The results of this comparison can be observed in Figure 5. As this figure shows, a very good conformation exists between the results which show a promising performance of the current method for non-Newtonian fluid flow simulations.

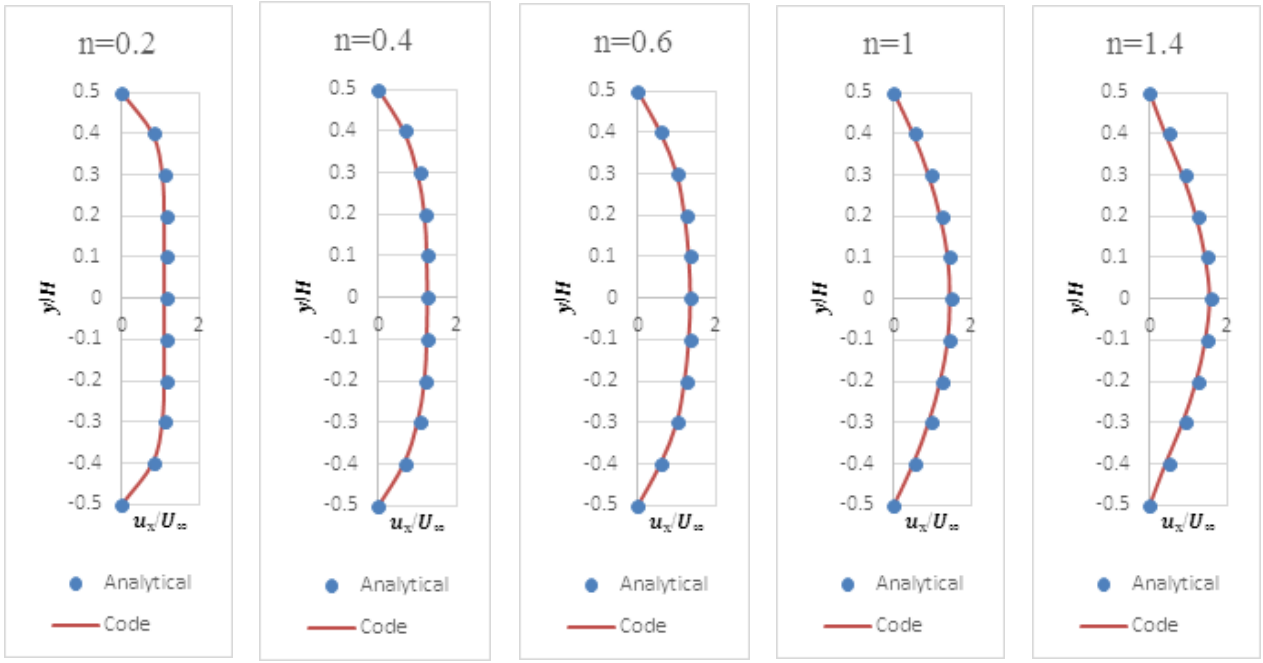

Figure 3. Comparison of the analytical solution and the present results of RVM for a non-Newtonian flow between two infinite parallel flat plates with different power-law indexes

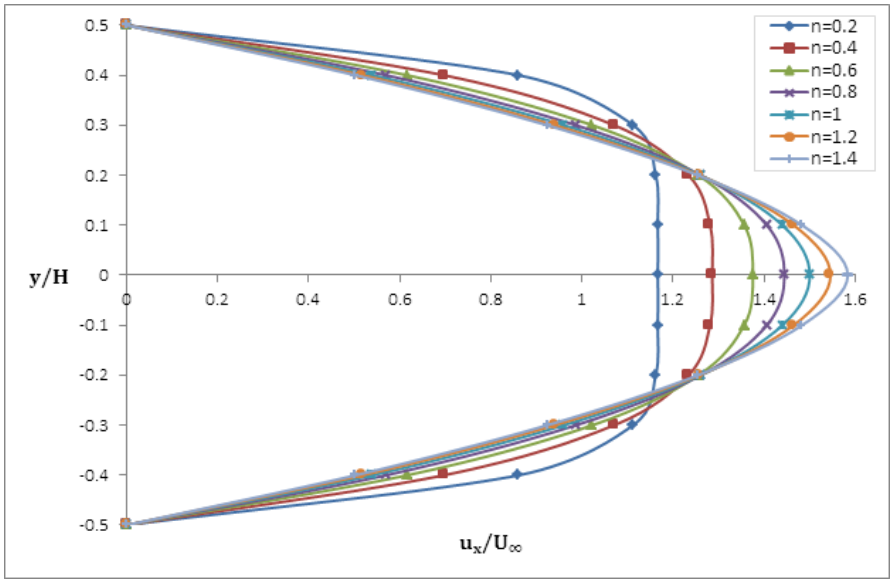

Figure 4. Horizontal velocity profiles of non-Newtonian fluid flow between two infinite parallel flat plates with different power-law indexes (Obtained from present study)

For n=0.2, 0.4, 0.6 and 1, the minimum percentage of deviation of the values obtained in present study in comparison with the outcomes of Khandelwal et al. [13] were about 0.41%, 0.26%, 0.56% and 0%, respectively; while the maximum deviations were about 5.17%, 2.45%, 1.61% and 2.93%, respectively.

Furthermore, for n=1, the minimum percentage deviation of the values in comparison with the results of Hayes et al. [12] is about 0.29%; while the maximum deviation is about 3.87%. As the figure shows, there is an acceptable conformation between the present study results and the both sets of results.

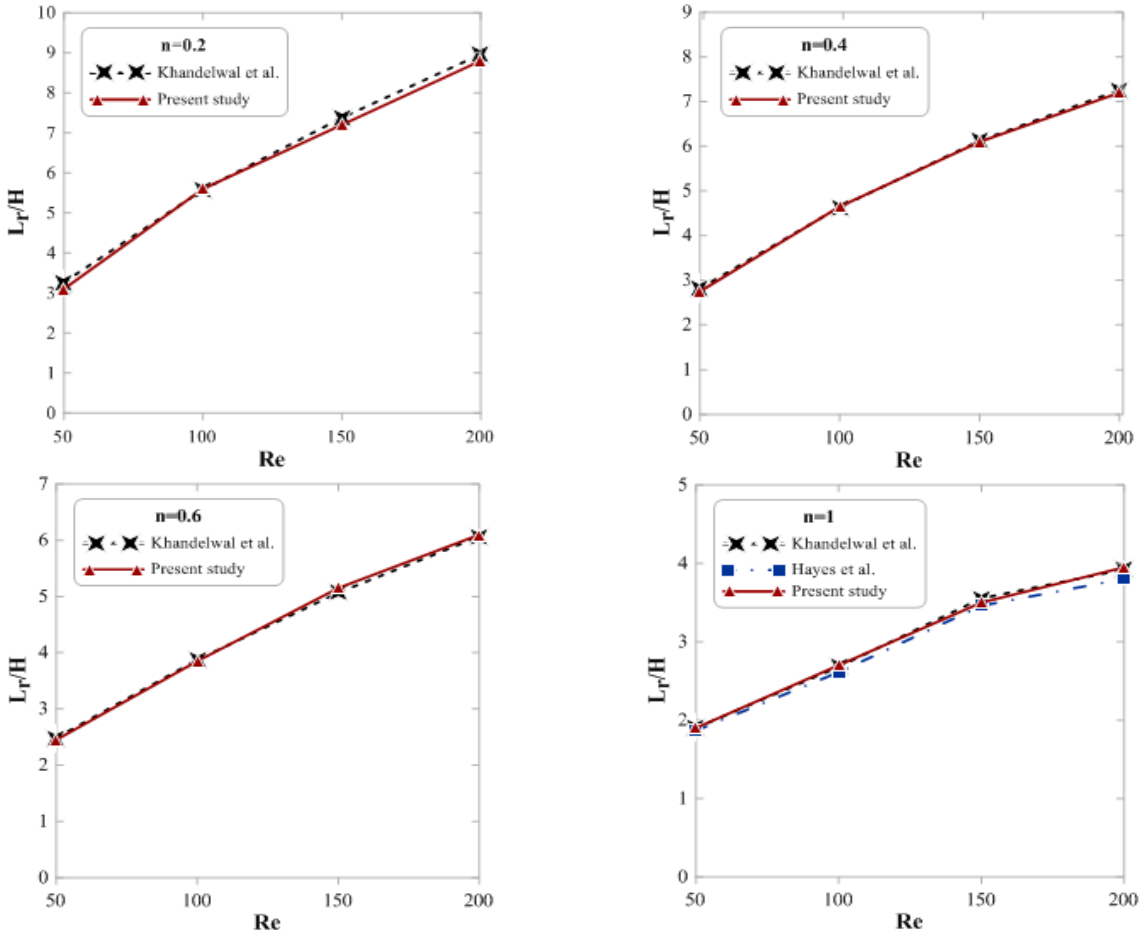

Figure 5. Comparison of recirculation length (L_r/H) with that of Khandelwal et al. [13] for n=0.2,0.4,0.6 and with that of Khandelwal et al. [13] and Hayes et al. [12] for n=1 at different values of Re

5. RESULTS AND DISCUSSION

The computation begins with the initial condition of the potential flow. Starting with a potential flow, the flow develops by generating vorticity along solid walls to annihilate the slip velocity. The vortexes motion stems from both convection and diffusion mechanisms. Vortexes that move away from the computational domain are neglected in the computational process.

Once the vortexes fill all the computing domain, their number is almost constant; which means: $\frac{dN}{dt} \approx 0$ (N is the total number of vortexes within the computing domain). Afterwards, velocity can be evaluated anywhere in the flow. Such a velocity field is instantaneous, and to obtain the average velocity, the computation must be repeated in several time steps and then averaged.

In order to investigate the effect of the parameters of power-law index and Reynolds number on the recirculation zone, after solving the non-Newtonian fluid flow using RVM, the streamlines inside the T-junction can be drawn. Figure 6 illustrates the streamlines inside a T-junction for *Re=50, 100, 150* and *200*, respectively. To demonstrate the effect of the power-law index over the flow, seven cases (*n=0.2, 0.4, 0.6, 0.8, 1, 1.2 and 1.4*) are investigated, which is shown here as an example of one case (*n=0.2*). This figure shows that for a specific power-law index, increasing the Reynolds number increases the length of the recirculation zone.

Figure 7 shows the streamlines inside a T-junction for *n=0.2, 0.4, 0.6, 0.8, 1* and *1.2*, respectively for four fixed Reynolds numbers *Re=50, 100, 150* and *200* (here for *Re=100*). The results show that, by increasing the value of the power-law index, the length of the recirculation zone decreases. This is due to that by increasing the power-law index, the local Reynolds number decreases in the whole flow field. In other words, with increasing the power-law index, the shear thickening treatment of the fluid rises and as a consequence, the fluid viscosity grows higher which leads to a decrease into the length of the recirculation zone.

After finding the length of the recirculation zone in the lateral branch for different values of the Reynolds number and the power-law indexes, these values can be displayed on a graph to compare results. Figure 8 illustrates the length of the recirculation zone within the T-junction in terms of the Reynolds number for the various power-law indexes. For a particular power-law index, this length increases nonlinearly with increasing Reynolds number. Also, for a fixed Reynolds number, the recirculation length increases with decreasing power-law index. Therefore, it can be concluded that the recirculation length is a function of the power-law index and the Reynolds number. Another important conclusion that can be drawn from this figure is that the lower the power-law index, the greater the effect of the Reynolds number on the length of the recirculation zone. In contrast, increasing the Reynolds number for the power-law indexes with high values does not have a significant effect on the length of the recirculation zone.

It is important to determine the critical Reynolds number in which the start of the recirculation zone appears in the lateral branch, is very important. In present study critical Reynolds numbers are obtained for several of the power-law indexes. For this purpose, for a specific power-law index, the Reynolds number is gradually increased from the lower values with a tolerance of ±1, and for each value of the Reynolds number, the change of the velocity sign in the y-direction inside the lateral branch is checked. The change in the velocity sign indicates the presence of a recirculation zone there. For instance, Figure 9 illustrates the streamlines in a T-junction for the critical Reynolds number for the cases of n=0.2 and 1.2, respectively. As can be seen from this figure, for n=0.2, up to Re=8, no sign change in velocity and therefore no wake is observed in the flow, but as the Reynolds number increases to Re=9, a recirculation zone in the lateral branch appears. In the same way, for n=1.2, no recirculation zone exists until Re=19 but this zone appears at Re=20.

Figure 10 illustrates the critical Reynolds number in terms of power-law index obtained from present study in comparison with the results of Khandelwal et al. [13]. As the figure shows, there is very good conformation between both sets of results. By incrementing the power-law index, the critical Reynolds number is enhanced, meaning that the start of the recirculation zone appearing in the lateral branch occurs at a higher Reynolds number. In the other words, with increasing the power-law index, the shear thickening treatment of the fluid rises and as a consequence, the fluid viscosity grows higher which leads to recirculation zones occurring at a higher Reynolds number.

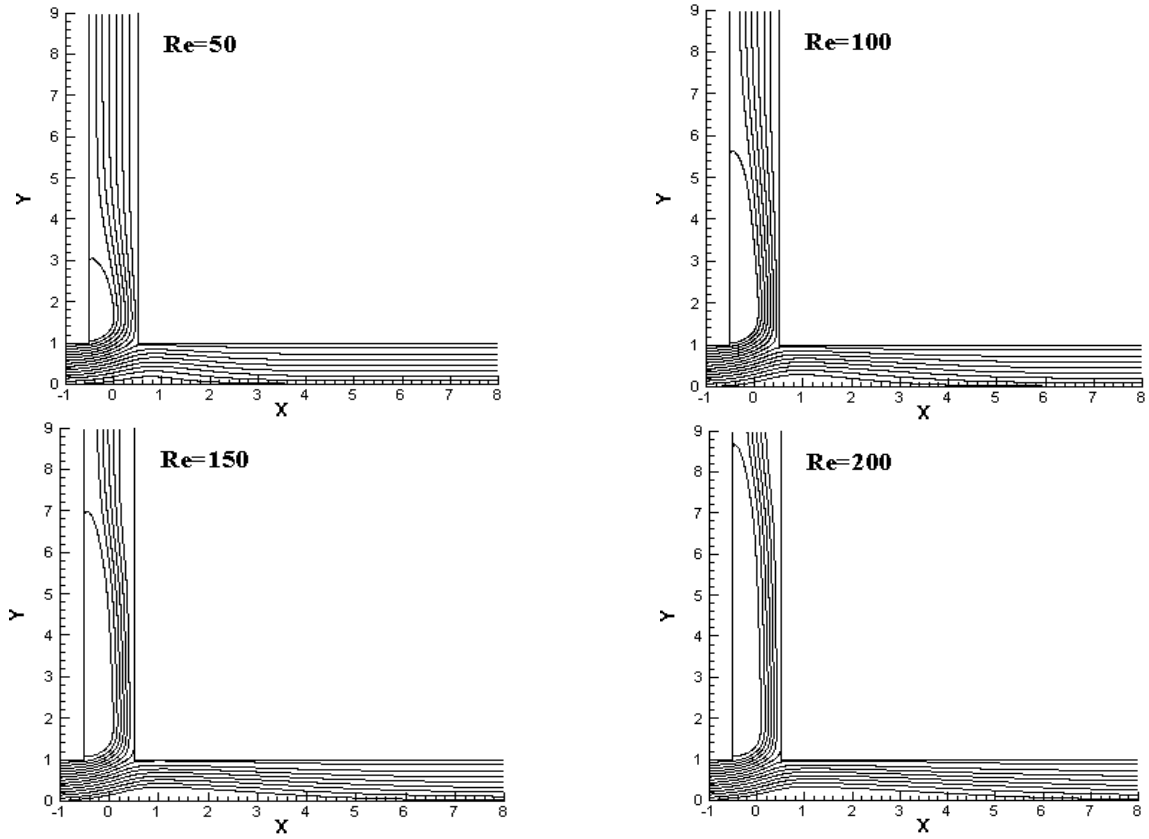

Figure 6. Streamlines inside a T-junction at different values of Re for n=0.2 (Obtained from present study)

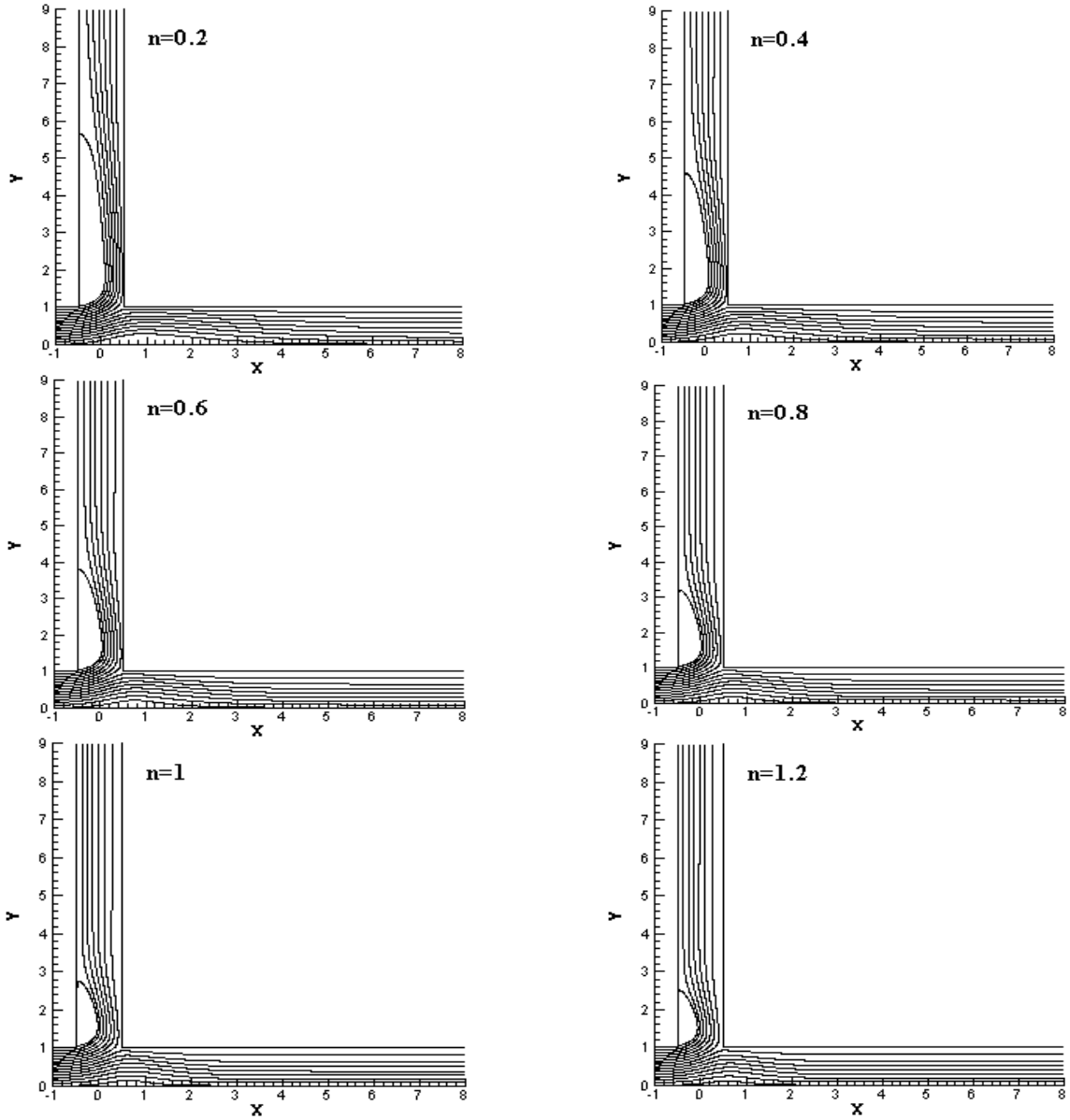

Figure 7. Streamlines inside a T-junction at different values of n for Re=100 (Obtained from present study)

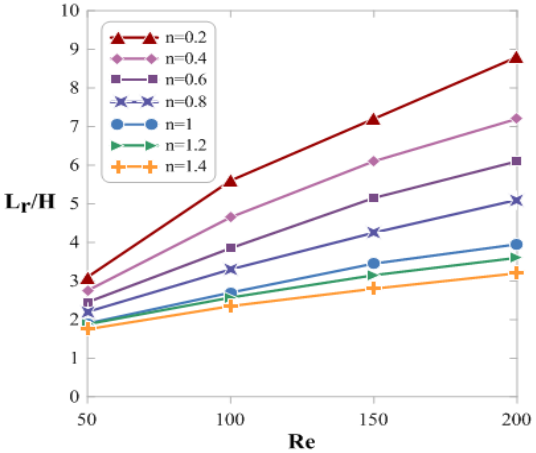

Figure 8. Variation of recirculation length (L_r/H) with Re at different values of power-law indexes (Obtained from present study)

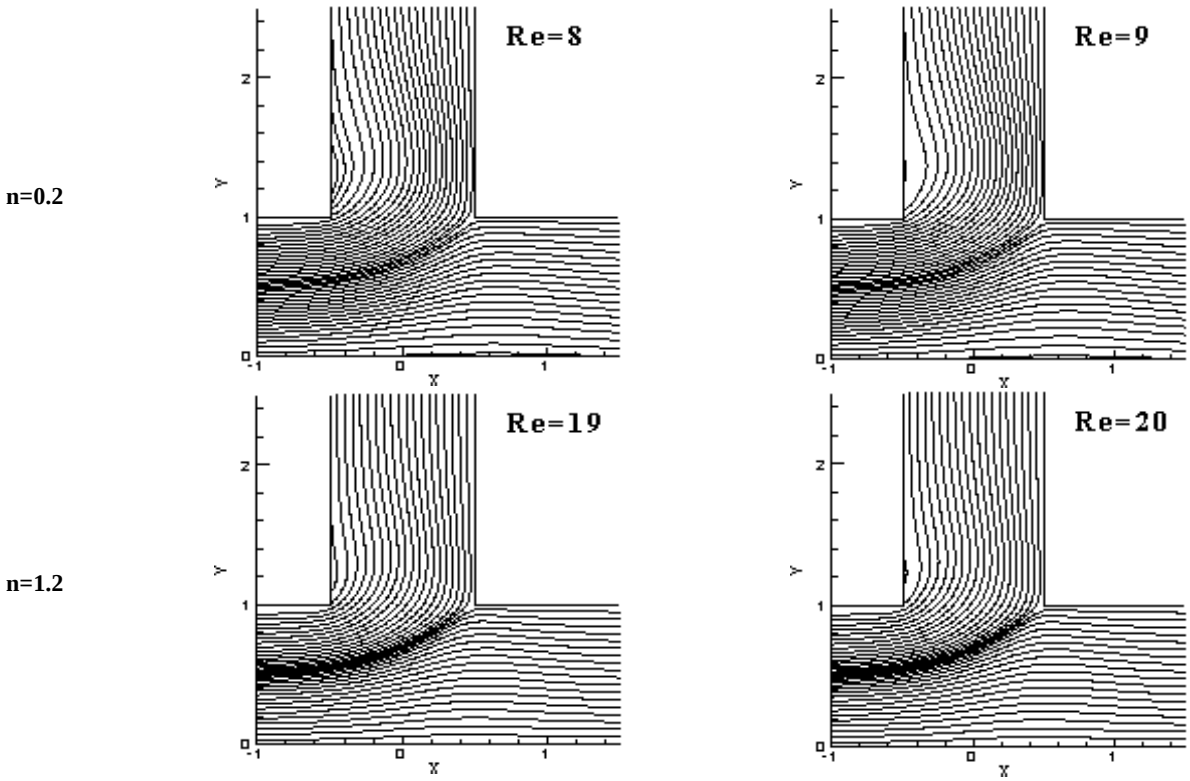

Figure 9. Streamlines for critical Reynolds number in which the start of the recirculation zone appears in the side branch for n=0.2 and 1.2 (Obtained from present study)

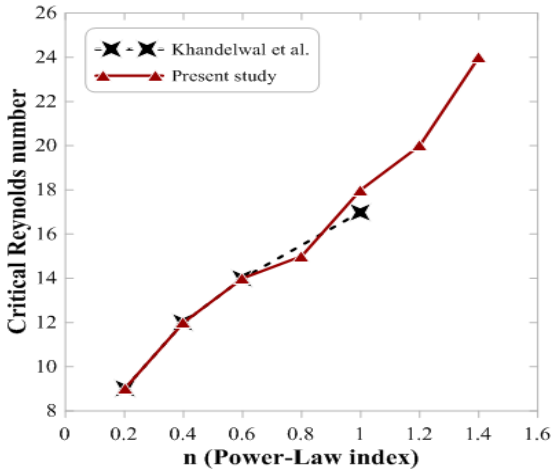

Figure 10. Comparison of critical Reynolds number for the onset of flow separation at different values of power-law indexes with that of Khandelwal et al. [13]

6. CONCLUSION

As mentioned earlier, the main purpose of this study is to develop the Random Vortex Method in simulating and solving the flow of non-Newtonian fluids, which in this research is offered for the first time with the introduction of a new approach. By observing the obtained results and comparing them with the numerical and experimental results of other researchers, there is a very good and acceptable agreement, which proves that the proposed method is very capable in simulating the flow of non-Newtonian fluids. Therefore, from now on, the RVM can be considered as one of the reliable and accurate methods in non-Newtonian fluid analysis and many existing non-Newtonian fluid problems can be investigated by this method.

Important advantages of the RVM include its ability to study the fluid flow in a wide range of Reynolds numbers, including laminar and turbulent regimes, solving time-based equations, and no need to simplify governing equations. Therefore, this method can be used for two-phase flows that need to determine the instantaneous velocities. Also, simulation of turbulent flow in this method is possible easily and with very high accuracy and can be considered as future work. In addition to internal flows, this method can also be used to simulate external flows.

In conclusion, it can be said that in this study, the capability of the RVM in simulating and solving the flow of non-Newtonian fluids has been proven. Therefore, it is suggested that other studies be performed to investigate the flow of non-Newtonian fluids with this method, especially the simulation of turbulent flows, which this method is able to solve with high accuracy.

7. REFERENCES

1. Yang, B., Su, W., Deng, Sh., Zhao, L., Lu, P., "State-of-art of impacting T-junction: Phase separation, constituent separation and applications", ***International Journal of Heat and Mass Transfer***, Vol. 148, (2020), 119067. DOI: https://doi.org/10.1016/j.ijheatmasstransfer.2019.119067
2. Chorin, A. J., "Numerical study of slightly viscous flow", ***Journal of Fluid Mechanic***, Vol. 57, (1973), 785-796. DOI: https://doi.org/10.1017/S0022112073002016
3. Chorin, A. J., "Vortex sheet approximation of boundary layers", ***Journal of Computational Physics***, Vol. 27, (1978), 428-442. DOI: https://doi.org/10.1016/0021-9991(78)90019-0
4. Gagnon, Y., Giovannini, A., "Numerical simulation and physical analysis of high Reynolds number recirculating flows behind sudden expansions", ***Journal of Physics Fluids***, Vol. 5, (1993), 2377-2389. DOI: https://doi.org/10.1063/1.858752
5. Noori, Y., Zafarmand, B., "Simulating of laminar and turbulent flows inside diverging channels with Random Vortex Method (RVM) and investigating the effects of the angle of divergence and the Reynolds number on the recirculating flow inside the channels", ***Journal of Applied and Computational Sciences in Mechanics***, Vol. 26, (2015), 17-34. DOI: 10.22067/fum-mech.v26i1.23642
6. Zafarmand, B., Souhar, M., Hossein Nezhad, A., "Analysis of the characteristics, physical concepts and entropy generation in a turbulent channel flow using Vortex Blob Method", ***International Journal of Engineering, Transactions B: Applications,*** Vol. 29, No. 7, (2016), 985-994. DOI: 10.5829/idosi.ije.2016.29.07a.14
7. Zafarmand, B., Ghadirzad, N., "High Reynolds viscous flow simulation past the elliptical Airfoil by Random Vortex Blob", ***International Journal of Engineering, Transactions B: Applications,*** Vol. 30, No. 12, (2017), 1903-1910. DOI: 10.5829/ije.2017.30.12c.12
8. Tadayoni Navaei, I., Zafarmand, B., "Random Vortex Method for Geometries with Unsolvable Schwarz-Christoffel Formula", ***International Journal of Engineering, Transactions B: Applications,*** Vol. 31, No. 1, (2018), 38-44. DOI: 10.5829/ije.2018.31.01a.06
9. Jin, G., Zou, L., Jiang, Y., Zong, Z., Sun, Z., "A circle theorem technique to handle 2-D flows around arbitrary cylinders in discrete vortex method", ***Journal of Wind Engineering & Industrial Aerodynamics***, Vol. 209, (2021), 104496. DOI : https://doi.org/10.1016/j.jweia.2020.104496
10. Mimeau, Ch., Marie, S., Mortazavi, I., "A comparison of semi-Lagrangian vortex method and lattice Boltzmann method for incompressible flows", ***Computers and Fluids***, Vol. 224, (2021), 104946. DOI :https://doi.org/10.1016/j.compfluid.2021.104946
11. Qian, Z., Yao, Y., "McKean–Vlasov type stochastic differential equations arising from the random vortex method", ***Partial Differential Equations and Applications***, Vol. 3, No. 1, (2021). DOI: https://doi.org/10.1007/s42985-021-00146-z
12. Hayes, R. E., Nandakumar, K., Nasr-El-Din, H., "Steady laminar flow in a 90 degree planar branch", ***Computers and Fluids***, Vol. 17, (1989), 537-553. DOI :https://doi.org/10.1016/0045-7930(89)90027-3
13. Khandelwal, V., Dhiman, A., Baranyi, L., "Steady laminar flow in a 90 degree planar branch", ***Computers and Fluids***, Vol. 17, No. 4, (2014). DOI : http://dx.doi.org/10.1016/j.compfluid.2014.11.030
14. Brandi, A.C., Mendonca, M.T., Souza, L.F., "DNS and LST stability analysis of Oldroyd-B fluid in a flow between two parallel plates", ***Journal of Non-Newtonian Fluid Mechanics***, Vol. 267, (2019). DOI: https://doi.org/10.1016/j.jnnfm.2019.03.003
15. Zhou, H., Zhu, Ch., Fu, T., Ma, Y., Li, H. Z., "Dynamics and interfacial evolution for bubble breakup in shear-thinning non-Newtonian fluid in microfluidic T-junction", ***Chemical Engineering Science***, Vol. 208, (2019), 115-158. DOI: https://doi.org/10.1016/j.ces.2019.115158
16. Kwak, H., Nam, J., "Simple criterion for vortex formation in the channel flow of power-law fluids", ***Journal of Non-Newtonian Fluid Mechanics,*** Vol. 284, (2020). DOI: https://doi.org/10.1016/j.jnnfm.2020.104372
17. Luo, H., Delache, A., Simoens, S., "Mixing of non-Newtonian inelastic fluid in a turbulent patch of T-junction", ***Journal of Non-Newtonian Fluid Mechanics***, (2020). DOI: https://doi.org/10.1016/j.jnnfm.2020.104307
18. Yang, B., Deng, Sh., Sub, W., Zhao, L., Wang, D., "Experimental investigation on phase separation comparison between single and double T-junctions", ***Experimental Thermal and Fluid Science,*** Vol. 118, (2020). DOI: https://doi.org/10.1016/j.expthermflusci.2020.110171
19. Rostami, B., Morini, G. L., "Generation of Newtonian droplets in Newtonian and non-Newtonian carrier flows in micro T-junctions under opposed-flow configuration", ***Journal of Non-Newtonian Fluid Mechanics***, Vol. 281, (2020). DOI: https://doi.org/10.1016/j.jnnfm.2020.104297
20. Moghimi, S. M., Abbasi, M., Khaki Jamei, M., Domirri Ganji, D., "Effect of Non-uniform Magnetic Field on Non-newtonian Fluid Separation in a Diffuser", ***International Journal of Engineering, Transactions A: Basics,*** Vol. 33, No. 7, (2020), 1354-1363. DOI: 10.5829/ije.2020.33.07a.23
21. Maurya, A., Tiwari, N., Chhabra, R.P., "Controlling the flow and heat transfer characteristics of power-law fluids in T-junctions using a rotating cylinder", ***International Journal of Thermal Sciences***, Vol. 163, (2021). DOI: https://doi.org/10.1016/j.ijthermalsci.2021.106854
22. Motahar, S., "A Neural Network Approach to Estimate Non-Newtonian Behavior of Nanofluid Phase Change Material Containing Mesoporous Silica Particles", ***International Journal of Engineering, Transactions B: Applications,*** Vol. 34, No. 8, (2021), 1974-1981. DOI: 10.5829/ije.2021.34.08b.18
23. Vatani, M., Domirri Ganji, D., "Experimental Examination of Gas-liquid Two-phase Flow Patterns in an Inclined Rectangular Channel with 90° Bend for Various Vertical Lengths", ***International Journal of Engineering, Transactions A: Basics,*** Vol. 35, No. 4, (2022), 685-691. DOI: 10.5829/ije.2022.35.04a.07
24. Streeter, V. L., Wylie, E. B., K. Bedford, W., "Fluid Mechanics", 9th Edition, W.C. Brown Pub. Co, ISBN-13: 978-0070625372, (1997).
25. Nehari, Z., "Conformal Mapping", New York, McGraw-Hill, ISBN 978-0-486-61137-2, (1952).
26. Chhabra, R. P., Richardson, J. F., "Non-Newtonian Flow and Applied Rheology", Second Edition, ISBN 978-0-7506-8532-0, (2008). DOI: https://doi.org/10.1016/B978-0-7506-8532-0.X0001-7
27. Polyanin, A. D., "Handbook of Linear Partial Differential Equations for Engineers and Scientists", Chapman and Hall/CRC, Edition, ISBN 978-1-58488-299-9, (2002).
28. Rakotomalala, N., Salin, D., Watzky, P., "Simulations of viscous flows of complex fluids with a Bhatnagar, Gross, and Krook lattice gas", ***Physics of Fluids,*** Vol. 8, (1996). DOI: https://doi.org/10.1063/1.869093

Persian Abstract

چکیده

مطالعات گذشته نشان می دهد که تاکنون از روش ورتکس های تصادفی (RVM) فقط برای حل جریان سه یالات نیوتنی استفاده می شده است. در این مقاله با ارائه یک رویکرد جدید، روش ورتکس های تصادفی برای اولین بار با هدف شبیه سازی جریان سه یالات غیر نیوتنی توسعه داده شده است. برای این منظور، جریان دوبعدی سه یال غیرنیوتنی پاورلا در یک اتصال T به صورت عددی شبیه‌سازی شده است. این شبیه سازی برای عدد رینولدز ورودی کانال در محدوده Re = 50-200 و شاخص های مختلف پاورلا در طیف n = 0.2-1.4 انجام شده است. روش ورتکس های تصادفی معادلات ناویر-استوکس را به صورت تابعی از زمان حل می کند و بدون نیاز به شبکه بندی بر روی هندسه و همچنین بدون نیاز به تعیین سرعت در تمام میدان سیال، سرعت در هر نقطه از کانال را تعیین می نماید. سرعت پتانسیل به عنوان شرط اولیه در تحلیل جریان به روش ورتکس های تصادفی است که در این مقاله با استفاده از تبدیل همدیس شوارتز-کریستوفل به دست آمده است. اثر دو پارامتر شاخص پاورلا و عدد رینولدز بر ناحیه گردش مجدد بررسی شده است. توافق قابل قبول بین نتایج مطالعه حاضر و نتایج عددی و تجربی موجود، قابلیت روش ارائه شده را نشان می‌دهد که با توجه به آن می توان روش ورتکس های تصادفی را یک روش امیدوارکننده قدرتمند در شبیه‌سازی جریان سیالات غیرنیوتنی در رژیم های جریان آرام و درهم در نظر گرفته گرفت.